Virology 380 (2008) 157–163

Contents lists available at ScienceDirect

Virology

journal homepage: www.elsevier.com/locate/yviro

The effect of point mutations within the N-terminal domain of Mason-Pfizer monkey virus capsid protein on virus core assembly and infectivity

Marcela Wildová [a], Romana Hadravová [a], Jitka Štokrová [a], Ivana Křížová [a], Tomáš Ruml [a,b], Eric Hunter [c], Iva Pichová [a,*], Michaela Rumlová [a,b,*]

[a] Gilead Sciences and IOCB Research Centre, Institute of Organic Chemistry and Biochemistry, Academy of Sciences of the Czech Republic, Flemingovo nám. 2, 166 10, Prague, Czech Republic
[b] Department of Biochemistry and Microbiology and Center of Applied Genomics, Institute of Chemical Technology, Prague, Technická 3, 166 28 Prague, Czech Republic
[c] Yerkes Natural Primate Research Center, Emory Vaccine Center, 954 Gatewood Road, Atlanta GA 30329, USA

ARTICLE INFO

Article history:
Received 20 June 2008
Returned to author for revision 10 July 2008
Accepted 22 July 2008
Available online 27 August 2008

Keywords:
Retrovirus
Assembly
Capsid protein
M-PMV
β-hairpin

ABSTRACT

Retroviral capsid protein (CA) mediates protein interactions driving the assembly of both immature viral particles and the core of the mature virions. Structurally conserved N-terminal domains of several retroviruses refold after proteolytic cleavage into a β-hairpin, stabilized by a salt bridge between conserved N-terminal Pro and Asp residues. Based on comparison with other retroviral CA, we identified Asp50 and Asp57 as putative interacting partners for Pro1 in Mason-Pfizer monkey virus (M-PMV) CA. To investigate the importance of CA Pro1 and its interacting Asp in M-PMV core assembly and infectivity, P1A, P1Y, D50A, T54A and D57A mutations were introduced into M-PMV. The P1A and D57A mutations partially blocked Gag processing and the released viral particles exhibited aberrant cores and were non-infectious. These data indicate that the region spanning residues Asp50–Asp57 plays an important role in stabilization of the β-hairpin and that Asp57 likely forms a salt-bridge with P1 in M-PMV CA.

Introduction

Assembly of retroviruses is driven by polymerization of Gag polyproteins, either at the plasma membrane (lentiviruses, alpha-viruses, gammaretroviruses) or at a distinct place within the infected cells (betaretroviruses). Immature spherical particles bud through the plasma membrane and the viral protease concomitantly cleaves Gag polyprotein precursors into discrete proteins. Three of these structural proteins, matrix (MA), capsid (CA) and nucleocapsid (NC) are common to all retroviruses and rearrange to form the mature, infectious virion. In mature virions the MA remains associated with the viral membrane and CA forms a protein shell surrounding a viral genomic RNA and NC complex.

During the assembly of immature viral particles the CA domain is thought to mediate Gag–Gag interactions (Gamble et al., 1997; Ganser-Pornillos et al., 2004; Kingston et al., 2000; Mortuza et al., 2004; von Schwedler et al., 2003). Although retroviral CA proteins exhibit a significant sequence similarity only in a short domain known as the major homology region, all high-resolution 3-D retroviral CA structures solved to date are remarkably similar (Gamble et al., 1996; Campos-Olivas et al., 2000; Jin et al., 1999; Khorasanizadeh et al., 1999; Gamble et al., 1997; Gitti et al., 1996; Kingston et al., 2000; Cornilescu et al., 2001; Mortuza et al., 2008). The capsid proteins are composed of two independently folded domains that are connected by short flexible linkers (Gamble et al., 1996; Momany et al., 1996; Gitti et al., 1996). The N-terminal domain (NTD) is composed of a β-hairpin followed by seven α-helices and the C-terminal dimerization domain (CTD) consists of four α-helices. All mature retroviral capsids except that of foamy virus contain N-terminal β-hairpin loops (HIV-1 (Human immunodeficiency virus) Pro1-Gln13, RSV (Rous sarcoma virus) Pro1-Thr12, and MLV (Murine leukemia virus) Pro1-Trp13). These loops are formed upon capsid maturation, during which cleavage releases the imino-group of Pro1, which is stabilized by formation of a salt bridge with a highly conserved aspartate (in HIV-1, RSV, MLV) or glutamate (in BIV, EIAV) (von Schwedler et al., 1998). Point mutations throughout this region block the *in vitro* assembly of HIV-1 capsid protein, HIV-1 core assembly *in vivo* and infectivity of HIV-1 (Abdurahman et al., 2007; Gross et al., 1998; Leschonsky et al., 2007; von Schwedler et al., 1998). A high-resolution structure of MLV capsid hexameric amino-terminal domain revealed that β-hairpins from each monomer are located at the center of the hexamer and form the wall of the central channel together with residues 14–16, thereby stabilizing and orienting residues involved in inter-subunit contacts (Mortuza et al., 2004). Recently, using electron microscopy and image reconstruction, it was confirmed that the hexameric rings are formed by CA-NTDs and stabilized by

* Corresponding authors. I. Pichová is to be contacted at fax: +420 220183556. M. Rumlová, Department of Biochemistry and Microbiology and Center of Applied Genomics, Institute of Chemical Technology, Prague, Technická 3, 166 28 Prague, Czech Republic. Fax: +420 220183556.
E-mail addresses: pichova@uochb.cas.cz (I. Pichová), rumlova@uochb.cas.cz (M. Rumlová).

0042-6822/$ – see front matter © 2008 Elsevier Inc. All rights reserved.
doi:10.1016/j.virol.2008.07.021

intermolecular interactions between helices 1–3 (Ganser-Pornillos et al., 2007).

Mason-Pfizer monkey virus (M-PMV), a member of the betaretrovirus family, assembles its immature capsids in the cytoplasm. After proteolytic cleavage the Gag polyprotein yields six structural proteins MAp10, phosphoprotein pp24, p12, CAp27, NCp14, and p4. Previous studies suggested that the N-terminal proline of M-PMV CA plays a key role in determining the particle shape. In *E. coli* the (ΔPro)CA-NC fusion protein lacking this P1 assembles into spherical particles rather than the sheets assembled by the CA-NC protein. Moreover, as with HIV (Gross et al., 1998; von Schwedler et al., 1998), merely extending the N-terminus of M-PMV CA by one amino acid is sufficient to induce the assembly of spherical particles (Rumlova-Klikova et al., 2000).

In contrast to the extensive mutational analysis performed on HIV-1 CA, the only one work concerning M-PMV CA has been published (Strambio-de-Castillia and Hunter, 1992). In order to investigate the contribution of the N-terminal proline and its putative interacting partner to core formation, we generated a series of mutations either of the N-terminal proline (P1A, P1Y) or within the region where the putative salt-bridge formation might occur (D50A, T54A, D57A).

Here we report the necessity of both the N-terminal proline and the aspartate residue in position 57 of CA protein for proper processing of Gag polyprotein, viral core formation and infectivity. These results suggest that in M-PMV CA the N-terminal β-hairpin is most probably stabilized by a salt bridge between these two residues and that substitution of some amino acid residues in the proximity dramatically reduces the infectivity.

Results

Virus production and maturation

Based on our previous results on the role of the N-terminal proline residue of CA in directing particle shape (Rumlova-Klikova et al., 2000) and on analogies with other viruses, we hypothesized that M-PMV NTD CA is stabilized by an interaction with some of the inner aspartate residues. To verify this and to determine which residues in M-PMV NTD contribute to the formation and stabilization of the β-hairpin and thereby the intermolecular contacts between CA proteins, five M-PMV mutants were prepared and analyzed. Pro1 (P1), Asp50 (D50), and Asp57 (D57) were individually replaced with alanine residues. Moreover, threonine, located two amino acids upstream of the most conserved Asp retroviral residue in CA (T48 in HIV, T51 in HTLV-1, T64 in MMTV, T49 in EIAV), was also replaced with alanine (T54A). P1 was also mutated to tyrosine, since Tyr is known to be present in position P1 of protease recognition sites (Pettit et al., 2002). The phenotypic effects of these mutations were assayed in COS-1 cells transfected with the wild-type and mutant proviral constructs. The intracellular levels and ratios of polyprotein precursors $Pr78^{Gag}$, $Pr95^{Gag\text{-}Pro}$, and $Pr180^{Gag\text{-}Pro\text{-}Pol}$ synthesized during the pulse period were comparable for the wild-type and all the mutants (Fig. 1A). After a 4-h chase, the mature capsid protein (27 kDa) was the predominant band in all cell lysates, except that from cells expressing the D57A mutant, in which several distinct CA-related intermediates of approximate molecular weights 35, 40, and 48 kDa appeared (Fig.1B). The characteristic wild-type like processing pattern of Gag polyprotein was observed in released particles of the P1Y, D50A, and T54A mutants (Fig. 1C). The CA-related intermediates, identical to those detected in the cells transfected with the D57A mutant, were also present in released D57A mutant particles, and low amounts of these products were observed in P1A particles (Fig. 1C, lanes 4 and 8). Moreover, a capsid protein cleavage product of molecular weight 20 kDa was also detected in both P1A and D57A (Fig. 1C, lanes 4 and 8). Similar results indicating altered processing of the P1A and D57A mutants were obtained by Western blot analysis of viral particles released 48 h post-transfection (Fig. 2A, lanes 3 and 7). Western blots of these

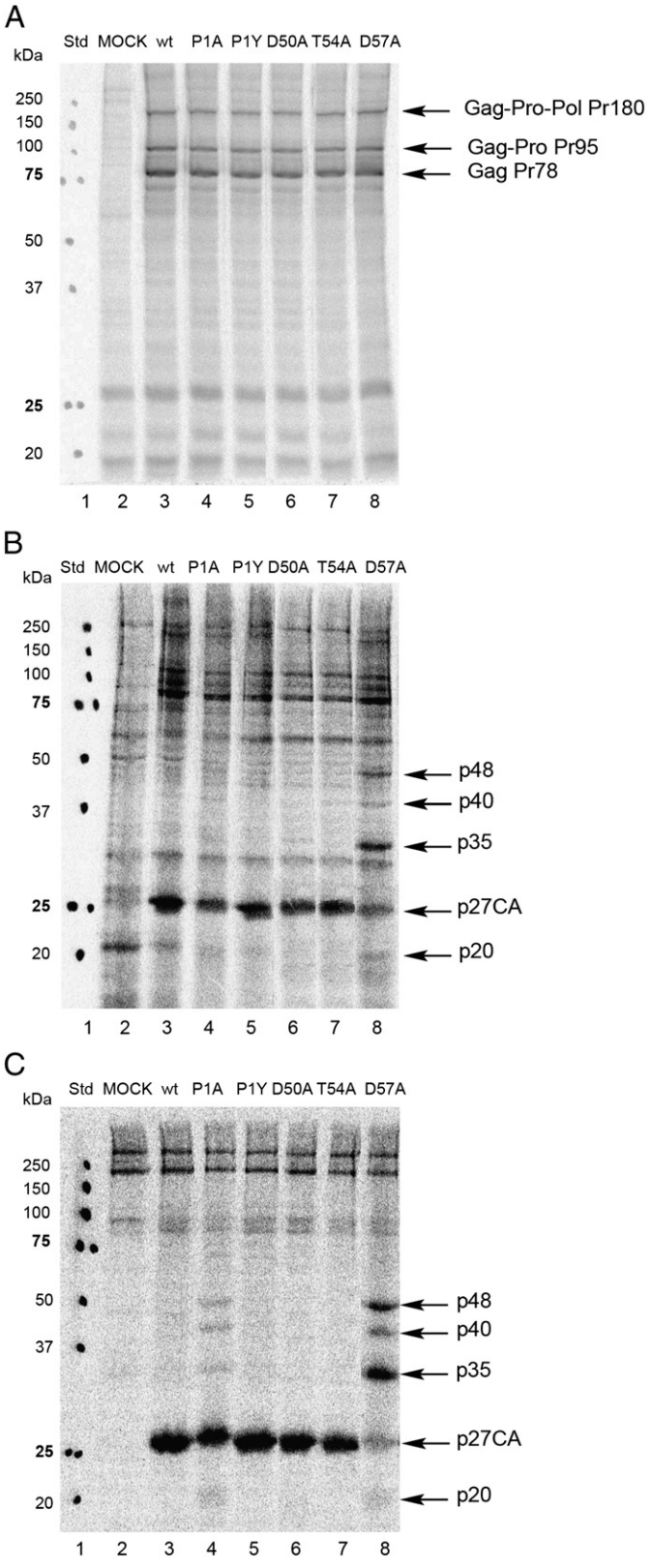

Fig. 1. Immunoprecipitation of cell- and virion-associated viral protein. COS-1 cells were transfected with wild-type or mutant proviral genome (P1A, P1Y, D50A, T54A, D57A). The cells were pulse-labeled with [^{35}S] methionine for 30 min (panel A) and chased for 4 h (B). The culture medium containing extracellular virions from the cells after a 4-h chase was filtered through a 0.45 μm filter (C). Viral-specific proteins were immunoprecipitated both from the cell lysates and culture media with a polyclonal rabbit anti-M-PMV CA antiserum. Proteins were separated on a 12% SDS-polyacrylamide gel. Molecular weight standards: 20, 25, 37, 50, 75, 100, 150 and 250 kDa.

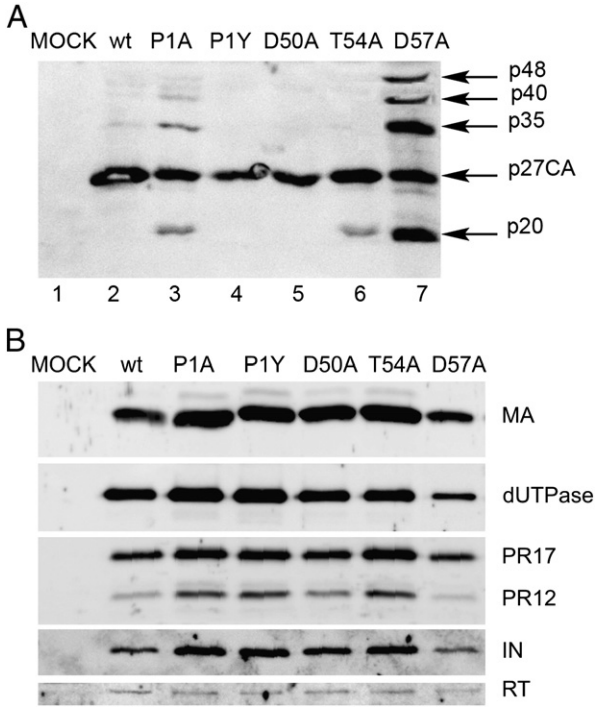

Fig. 2. Western blot analysis of released viruses. COS-1 cell were transfected with wild-type or mutant proviral DNAs. Viruses were harvested 48 h post-transfection and pelleted through a 20% sucrose cushion. The viral pellets were resuspended in protein loading buffer. Proteins were resolved using SDS-PAGE, and M-PMV related proteins were detected by rabbit antibodies against CA (A) and MA, dUTPase, PR, RT and IN (B).

two mutants reproducibly showed multiple bands corresponding to the additional CA-derived proteins of higher molecular weights (35, 40, and 48 kDa) and to the truncated CA protein (molecular weight 20 kDa). For better characterization of these Gag-processing intermediates, Western blots of samples of the released particles 48 h post-transfection were probed with antibodies specific to MA, p12 and NC. Mature matrix protein of correct molecular weight (p10MA) was observed in all mutants in amounts similar to the wild-type and the anti-MA antibody did not react with any of Gag cleavage intermediates (Fig. 2B). The analysis of partially processed Gag revealed the presence of NC in all three intermediates, and the p12 protein was also found in the band corresponding to proteins of molecular weight 48 kDa. To analyze whether the processing of the Gag-Pro or Gag-Pro-Pol polyproteins was not affected, Western blot using antibodies against dUTPase, protease (PR17, PR12), reverse transcriptase (RT) and integrase (IN) was performed (Fig. 2B). No difference in the processing of Pro-Pol region was observed between the mutant and the wild-type viruses (Fig. 2B). According to this data we can surmise that the Gag-processing intermediates p35, p40, and p48 correspond to CA-NC, CA-NC-p4, and p12-CA-NC fusion proteins. The p20 protein was recognized by a monoclonal antibody against the C-terminal part of CA, suggesting that the internal cleavage of CA occurs within its N-terminal part. The altered cleavage pattern of mutants P1A and D57A (Fig. 2 lanes 3 and 7), both identified to have partially blocked Gag polyprotein processing and internal cleavage within CA, suggested a change in the overall fold of the CA and adjacent regions. The T54A mutation did not prevent processing of Gag polyprotein; however, a truncated 20 kDa form of CA was detected in the pelleted virus (Fig. 2, lane 6).

Kinetic analysis and processing of the wt and D57A mutant

Since the initial pulse–chase experiments presented in Fig. 1 addressed only a single time point and did not provide information on the efficiency of the processing or the rate of turnover of unprocessed intermediates, we performed time–course pulse–chase experiments with the wild-type and P1A, P1Y, D50A, T54A, and D57A mutant proviral constructs. Transfected COS-1 cells were metabolically labeled and chased for 1, 4, 8, and 24 h. The virus-specific proteins were immunoprecipitated using rabbit anti M-PMV CA antiserum, and the CA-related band intensities for p20CA, p27CA, p35CA, p40CA, and p48CA were quantified. The total amounts of released capsid proteins for each construct were considered to be the sums of the virus-associated p27CA (grey part of bars Fig. 3) and the improperly processed CA-related p20CA, p35CA, p40CA, and p48CA proteins (black part of bars Fig. 3). The relative amounts of released CA-related proteins of individual mutants were compared to that of the wild-type, which was regarded as 100%. The P1Y mutant was released with efficiency comparable to the wild-type (more than 90% of the wt); slightly lower efficiency (about 80%) was observed for the P1A mutant and about 70% wt efficiency was observed for the T54A, D50A, and D57A mutants. The release of the D57A mutant increased slower in comparison to that of the wild-type as after 8 h chase period only 40% of wt level of extracellular particles was observed; this level remained constant for an additional 16 h (data not shown). However, only about 15% of virus-associated capsid protein p27CA properly processed from Gag polyproteins was detected in the D57A mutant (see Fig. 3), and this ratio did not change over the time period of the experiment. Similarly, the amounts and proportions of CA to CA-related products of incomplete cleavage of the P1A, P1Y, D50A, and T54A Gag mutants did not change over the chase period, suggesting that these CA-related intermediates are not products of non-specific Gag degradation.

Infectivity

The infectivity was determined by a single-round infectivity assay using the EGFP protein as a reporter in an assay described by Stansell et al. (2007). The virus-like particles (VLPs) released from the transfected cells were normalized based on quantification of reverse transcriptase activity. According to this assay no significant differences among the wild-type and the mutant VLPs were observed, suggesting that both wild-type and mutant virus particles are released with similar efficiency. Equivalent amounts of VLPs were used for infection of fresh COS-1 and 293T cells. The multiplicity of infection was analyzed by flow cytometry 48 h post-infection. The

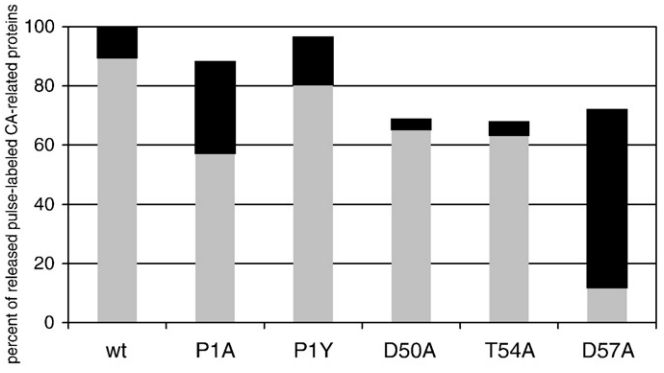

Fig. 3. Release and processing of wild-type and CA mutants. The percent of CA-related proteins released in the medium after a 4-h chase: p27CA (grey part of bars) and p20CA, p35CA, p40CA, and p48CA (black part of bars). COS-1 cells were transfected with wild-type or P1A, P1Y, D50A, T54A, or D57A mutant M-PMV proviral genome, metabolically labeled with [^{35}S] methionine, and immunoprecipitated from the medium 4 after chase. Proteins were separated by SDS-PAGE and the gel was imaged using phosphor screen (Typhoon). The quantification of CA-related band intensities for p27CA, p35CA, p40CA, p48CA, and p20CA was carried out using OptiQuant software. The sum of CA intensities of the wild-type virus was considered to be 100%.

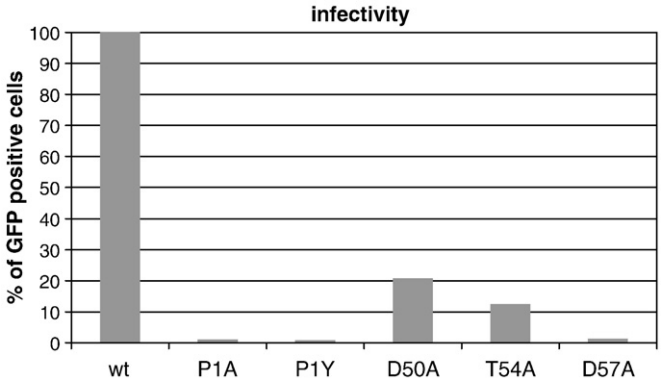

Fig. 4. Relative infectivity of M-PMV wild-type and P1A, P1Y, D50A, T54A, and D57A mutants analyzed by a single-round infectivity assay. COS-1 cells were transfected with the wild-type or mutant pSARM-EGFP and the pTMO vector. 48 h post-transfection the virions released into the media were filtered and normalized by RT assay. Equivalent amounts of virions were used for infection of fresh COS-1 cells. 48 h post-infection the percentage of GFP-expressing cells was determined by flow cytometry cell sorter analysis.

results from three independent infectivity determinations for the wild-type and the mutants are summarized in Fig. 4. The percentage of EGFP positive cells i.e. those infected with recombinant virus ranged between 30–35% for the wild-type and below 0.5% for the negative control. The relative infectivity for the wild-type was regarded as 100%. Interestingly, even the mutants D50A and T54A, which exhibited wild-type like kinetics of processing of Gag polyprotein, with the wild-type level of properly processed p27CA, showed a defect in the single-round infectivity assay and exhibited approximately 20% and 12% of the wild-type infectivity, respectively. The mutants with incomplete processing, P1A and D57A, and the P1Y mutant were non-infectious.

Particle morphology

The impaired processing of the P1A and D57A mutants, which do not yield mature p27CA, suggested that these mutations might affect mature core formation rather than the assembly of immature particles. To analyze this hypothesis, we carried out electron microscopic studies of thin sections of COS-1 cells transfected with the wild-type and mutant proviral constructs (Fig. 5). The overall appearance of the immature intracellular particles within the cells producing wild-type was very similar to those of the cells expressing the mutants. In these cells transfected with the wild-type, P1A, P1Y, D50A, T54A, and D57A mutants, both individual preassembled immature intracellular particles and clusters of particles accumulating at a distinct site in proximity to the nucleus and at the plasma membrane in the stage of budding were observed (data not shown). Released VLPs were observed for both wild-type and all mutants examined. The mutations P1Y, D50A, and T54A did not alter the viral particle morphology and the mature cores revealed the same size and shape as was observed for the wild-type (Fig. 5). In contrast, the mutants with affected Gag polyprotein processing showed defects in virus morphology. In the case of the P1A mutant oversized and mostly elongated particles with double or irregularly shaped cores were observed (Fig. 5). Similarly, released D57A particles did not contain characteristic cores; they harbored packed electron-dense material instead (Fig. 5). To compare the size and the density of these P1A and D57A aberrant VLPs to that of the wild-type, centrifugation in an iodixanol gradient was performed. First, the VLPs released from COS-1 cells expressing the wild-type, P1A, and D57A CA were concentrated from the media by sedimentation onto a 60% cushion of iodixanol. Next, the viral particles were separated by gradient centrifugation (continuous 10–40% iodixanol gradient) and their distribution was analyzed by Western blot. This experiment revealed that the wild-type and D57A VLPs sedimented at a density of 1.11–1.14 g/ml, whereas the P1A VLPs sedimented at a density of 1.13–1.15 g/ml. These

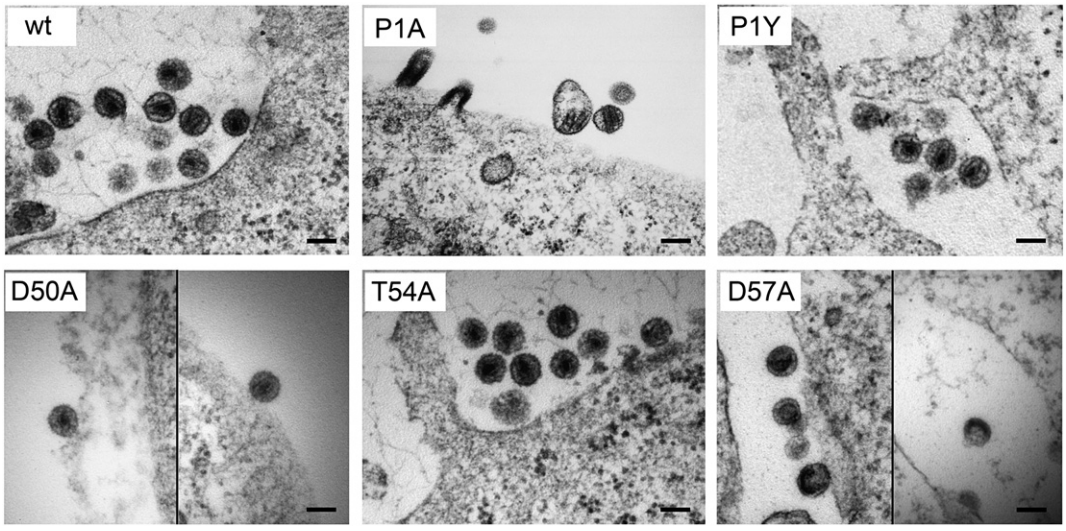

Fig. 5. Electron micrographs of the COS-1 cells expressing the wild-type and M-PMV CA mutants P1A, P1Y, D50A, T54A and D57A. Scale bars are 100 nm in all panels. Statistics data of observed particle is summarized below:

Construct	Number of immature intracytoplasmic particles	Mature particles	
		Regular particles/(%)	Irregular % (number)
Wild-type	104	64/(100)	0
P1A	14	2/(33)	4/(67)
P1Y	28	7/(100)	0
D50A	49	11/(85)	2/(15)
T54A	15	28/(100)	0
D57A	49	0	19/(100)

data are in an agreement with the EM observation, where VLPs released from the P1A expressing cells appeared to be larger in comparison to the wild-type and often contained double cores.

Discussion

As a result of processing, the N-terminal domain of retroviral CA refolds into a β-hairpin, stabilized by a salt bridge. This interaction is mediated by the N-terminal proline (Pro1) and an aspartate residue (Asp 51 in HIV-1 CA, Asp 52 in RSV, Asp 54 in MLV, Asp 54 in HTLV-1) that are both highly conserved among the retroviral CA proteins. M-PMV CA contains two potential candidates for the interaction with P1. Since the three-dimensional structure of M-PMV CA-NTD has not yet been solved, both D50 and D57 remain equally suitable partners for the interaction with Pro1 and stabilization of the β-hairpin.

Experiments with proviral M-PMV constructs showed that the levels of Gag polyprotein synthesized in transfected COS-1 cells were similar for all the mutants tested and did not differ from that seen with the wild-type. The Gag polyprotein in released particles was readily processed to effectively liberate its N-terminal MA protein, which was detected in all mutants and the wild-type. This was expected as previously described *in vitro* experiments simulating the activation of M-PMV protease demonstrated that M-PMV Gag processing is initiated by the liberation of matrix protein and phosphoprotein (pp24) (Parker and Hunter, 2001). In addition, it could be anticipated that structural changes in the CA domain would not affect the relatively distant cleavage at the N-terminus of Gag; in contrast to HIV-1, M-PMV MA is separated by two other proteins (pp24 and 12) from CA. In contrast to MA, the M-PMV CA protein was not released efficiently from wild-type Gag *in vitro* (Parker and Hunter, 2001). Moreover, the fusion protein CA-NC was not completely processed by M-PMV PR even during 48 h *in vitro* incubation (Rumlova et al., 2003). These results contrast with the *in vivo* experiments described in this work, in which complete processing of full length CA protein (p27) was observed both in the wild-type released particles and for the P1Y, D50A, and T54A mutants. However, in cells transfected with the P1A and D57A mutants the presence of persistent intermediates of Gag proteolytic processing was observed, indicating that D57A affects the accessibility of the p12/CA cleavage site. Comparison of the proteolytic products of P1Y and P1A justifies our assumption that tyrosine substitution for proline in the P1′ position will preserve the protease cleavage site. Indeed, this replacement (^{p12}PKDIF*PVTET^{CA}, ^{p12}PKDIF*YVTET^{CA}) had no effect on the proteolytic cleavage of mutated Gag polyprotein; the P1Y mutant underwent processing similar to that of the wild-type. The N- and C-terminally extended CA-related intermediates of Gag processing observed in the P1A and D57A mutants were identified as CA-NC (p35), CA-NC-p4 (p40) and p12-CA-NC (p48) using antibodies specific to M-PMV NC and p12. It is likely that preventing the proteolytic cleavage in p12*CA negatively affects further cleavage in CA*NC. This is consistent with the data published by Auerbach et al. (2007), who identified the Gag-processing intermediates as CA-NC, p12-CA-NC, and MA-p12-CA in MoMLV with an insertion mutation inhibiting the cleavage at the N-terminus of CA. In contrast to the D50A mutant, Western blots analyzing the P1A, T54A, and D57A M-PMV mutants revealed the presence of truncated CA protein in addition to the extended CA-related Gag cleavage products. Similarly, von Schwedler et al. (1998) observed multiple bands indicating a series of truncated p24CA molecules in released HIV-1 virions with D51A CA.

Mutational analyses of the N-terminal proline and its aspartate partner in HIV-1 (von Schwedler et al., 1998; Abdurahman et al., 2007; Leschonsky et al., 2007), MLV (Mortuza et al., 2004), MoMLV (Auerbach et al., 2007), and HTLV-1 (Bouamr et al., 2005; Rayne et al., 2001) showed the importance of the β-hairpin structure for stability, proper core formation and infectivity. Similarly, we describe here that both P1 and D57 mutations of M-PMV CA abolished the virus infectivity in 293T and COS-1 cells. EM analysis of the P1 and D57 mutants revealed aberrant cores in both mutant VLPs. The observation that although the P1Y, D50A, and T54A mutants exhibited reduced infectivity without impairing the processing, virus release and the mature core formation is puzzling. As the origin of reduced infectivity remains unclear and there is no detectable alteration in the virus life cycle, we can only speculate that the reasons could be e.g. an altered stability of the mature core, as reported for HIV-1 (Forshey et al., 2002) or a lack of some stabilization host cell factor.

Several pieces of evidence for the functional role of the conserved aspartate residues stabilizing the salt bridge between Pro1 and Asp of the CA-NTD are available (Bouamr et al., 2005; Mortuza et al., 2004; von Schwedler et al., 1998; von Schwedler et al., 2003). Bouamr et al. (2005) showed that D54A mutation in HTLV-1 CA did prevent neither correct proteolytic processing nor particle size and morphology. This contrasts to both HIV and M-PMV, where the D51A and D57A mutations, respectively, dramatically affected Gag polyprotein processing, core formation and infectivity. The D63A mutation of MMLV CA had also a dramatic effect on viral replication however, the infectivity and the capsid core formation were not studied in details (von Schwedler et al., 1998). Nevertheless, these data suggests a correlation of improper Gag cleavage with more dramatic changes inducing formation of differently shaped mature cores i.e. conical in lentiviruses (HIV-1), tubular in betaretroviruses (M-PMV) and spherical in gamma- and deltaretroviruses (MLV and HTLV-1, respectively). This is also in agreement with the observation that a block of the salt-bridge formation by masking of the Pro1 by short extensions of CA amino terminus i.e. four amino acids in HIV (von Schwedler et al., 1998; Gross et al., 1998), one in M-PMV (Rumlova-Klikova et al., 2000) and 25 in RSV (Nandhagopal et al., 2004) can switch the formation of tubular particles to the spherical. The fact that the assembly of spherical particles occurs also in the absence of β-hairpin indicates that the formation of a spherical core could be preferential to the formation of cones or tubes.

Materials and methods

Viral construct

All DNA manipulations were carried out using standard subcloning techniques, and plasmids were propagated in *E. coli* DH5α . All newly created constructs were verified by DNA sequencing. For cloning of viral constructs carrying point mutations a helper plasmid prepared by ligation of a SacI–PstI fragment corresponding to nucleotides 1163 to 3859 of M-PMV into SacI–NsiI pGEMEX-2 (Promega) was used as a template for oligonucleotide-directed mutagenesis. Primers were as follows 5′-CAAAAGATATTTTCGCCGTGACTGAAACC-3′ for introducing the *P1A* mutation, 5′-CAAAAGATATTTTCTATGTGACTGAAACC-3′ for *P1Y*, 5′-GGGGTAAGCCAATTAGCCGCTACAGATTCC-3′ for *D50A*, 5′-GGACAATTGGCTTGCCCCTACAGATTGG-3′ for *T54A* and 5′-TTACCCCTACAGCATGGAATACGC-3′ for *D57A*. SacI–Eco72I fragments of the helper plasmid carrying the point mutation within CA were ligated into the M-PMV proviral expression vector pSARM4.

For the infectivity assay the engineered M-PMV constructs were cloned into pSARM-EGFP via SacI and Eco72I (Newman et al., 2006).

Cell growth and virus production

COS-1 cells were grown in Dulbecco's modified Eagle medium (DMEM, Sigma) supplemented with 10% fetal bovine serum (Gibco) and 1% L-glutamine (PAA Laboratories, Linz, Austria). COS-1 cells were transfected with wild-type or mutant proviral DNA using Fugene 6 transfection reagent (Roche Molecular Biochemicals) according to the manufacturer's instructions. Supernatants were harvested 24, 48 or 72 h post-transfection and the viral pellet was obtained by centrifugation at 200,000x*g* for 1 h in a Beckman SW41Ti rotor. Protein expression was quantified using reverse transcriptase assay (RT) or Western blot.

Metabolic labeling and immunoprecipitation of Gag

COS-1 cells transfected with the appropriate DNA were grown for 48 h post-transfection, starved for 30 min in methionine and cysteine deficient DMEM (Sigma) and then pulse-labeled for 30 min with 125 μCi/ml of Tran^{35}S label (M.G.P., Czech Republic). The labeled cells were chased for an appropriate period of time. The cells from pulse and pulse–chase experiments were washed with cold phosphate-buffered saline (PBS), lysed in 1 ml of lysis buffer A (1% Triton X-100, 1% sodium deoxycholate, 0.05 M NaCl, 25 mM Tris, pH 8.0) on ice for 20 min and clarified by centrifugation at 13,000 ×*g* for 1 min. The culture medium of the chased cells was filtered through a 0.45 μm filter and SDS was added to a final concentration of 0.1%. Viral proteins were immunoprecipitated from the cells and culture media with a polyclonal rabbit anti-M-PMV CA antibody (dilution 1:1000) and separated by SDS-polyacrylamide gel electrophoresis (SDS-PAGE). Radiolabeled protein bands were quantified on a Packard Cyclone™ system using OptiQuant™ software (Perkin Elmer, Shelton, CT).

Isolation of the virus

VLPs released from the COS-1 cells expressing wild-type, P1A, or D57A mutants were filtered from the media through a 45 μm filter and concentrated by sedimentation onto a 1 ml 60% iodixanol cushion at 35,000 ×*g* for 1 h in a Beckman SW41Ti rotor. Supernatant containing VLPs from about 0.5 cm above the cushion was removed and layered onto a 10–40% of iodixanol gradient and centrifuged for 16 h at 35,000 ×*g* in a Beckman SW41Ti rotor. Individual fractions were analyzed by Western blot using anti-CA antibody.

Infectivity assay

COS-1 and 293T cells were transfected with both pSARM-EGFP, expressing either wild-type or mutant M-PMV *gag-EGFP* gene, and pTM0, expressing the M-PMV envelope glycoproteins (Newman et al., 2006; Brody and Hunter, 1992). Culture medium was harvested 48 h post-transfection, filtrated through a 0.45 μm filter, stabilized by addition of polybrene to a final concentration of 8 μg/ml, and analyzed for RT activity. Normalized amounts of virions from the RT activity assay were used for infection of COS-1 cells. After 2 h incubation the volume of the media was adjusted to 4 ml by complete DMEM and the cells were incubated for an additional 24, 48 or 72 h. The cells were fixed with 3% formaldehyde and the number of GFP positive cells was determined by flow cytometry (BD FACSaria).

Reverse transcriptase assay

Virions from 4 ml of filtered culture supernatant were pelleted by centrifugation at 200,000 ×*g* in a Beckman SW41Ti rotor for 1 h and the pellet was resuspended in 50 μl of buffer L (50 mM Tris pH 8, 100 mM KCl, 0.05% Nonidet NP-40, 2 mM DTT). The final RT sample consisted of 50 mM Tris pH 8, 90 mM KCl, 8 mM $MgCl_2$, 0.05% Nonidet NP-40, 0.3 μg dA oligo, 0.6 μg poly rU, 20 mM DTT and 10 μCi α^{33}P dATP. 10 μl of lysed virions was mixed with 40 μl of reaction mixture and incubated at 37 °C for 1 h. 5 μl was spotted on Whatman DE-81 paper, washed with SSC buffer (1.5 mM sodium citrate buffer pH 7 and 150 mM NaCl) and analyzed with a Typhoon Phosphoimager.

Western blotting

COS-1 cells were transfected with wild-type or mutant proviral constructs. Culture supernatant was harvested 48 h post-transfection, filtered through a 0.45-μm filter, and ultracentrifuged through a 20% sucrose cushion for 1 h at 200,000 ×*g* in a Beckman SW41Ti rotor. The pellet was resuspended in protein loading buffer and the proteins were separated by SDS-PAGE and blotted onto a nitrocellulose membrane. Membrane-bound CA-related proteins were immunodetected with a rabbit anti-M-PMV CA, MA, dUTPase, PR, IN and RT polyclonal antibodies. The blots were then incubated with secondary HRP-conjugated antibody and developed by chemiluminescent substrate (Pierce).

Electron microscopy of tissue culture cells

COS-1 cells transiently expressing the wild-type or mutant M-PMV proviral constructs grown on 60 mm plastic dishes were washed three times with PBS, scraped into a microtube and prefixed with freshly prepared 2.5% glutaraldehyde in 0.1 M cacodylate buffer pH 7.5. After washing with 0.1 M cacodylate buffer pH 7.5 the cells were postfixed in 1% osmium tetroxide, dehydrated in an ethanol series (30, 50, 70, 80, 90, and 100%) and embedded in fresh EMBED 812 or AGAR 100 epoxy resin in a labeled Beem capsule. Ultrathin sections (70 nm) of cells were cut with a diamond knife on a RMC MT 7000 Ultramicrotome and placed on 200-mesh copper grids. The sections were contrasted with uranyl acetate and lead citrate. A JEOL JEM-1200EX analytical transmission electron microscope operated at 60 kV was used for analysis.

Acknowledgments

We thank Jeannette Taylor from IM&MF in Emory University for technical assistance in the electron microscopic studies and Romana Cubínková from Gilead Sciences & IOCB Research Centre for excellent technical assistance. We also thank Ria Čechová, Jana Šípová and Hillary Hoffman for help in preparation of the manuscript. This work was supported by the "Centre for New Antivirals and Antineoplastics" 1M6138896301 of the programme of the Czech Ministry of Education, by research project Z40550506, 1M6837805002, MSM 6046137305 and by grants KAN208240651 and SCO/06/E001 (EUROCORES) from the Czech Science Foundation.

References

Abdurahman, S., Youssefi, M., Hoglund, S., Vahlne, A., 2007. Characterization of the invariable residue 51 mutations of human immunodeficiency virus type 1 capsid protein on in vitro CA assembly and infectivity. Retrovirology 4, 69.
Auerbach, M.R., Brown, K.R., Singh, I.R., 2007. Mutational analysis of the N-Terminal domain of Moloney murine leukemia virus capsid protein. J. Virol. 81, 12337–12347.
Bouamr, F., Cornilescu, C.C., Goff, S.P., Tjandra, N., Carter, C.A., 2005. Structural and dynamics studies of the D54A mutant of human T cell leukemia virus-1 capsid protein. J. Biol. Chem. 280, 6792–6801.
Brody, B.A., Hunter, E., 1992. Mutations within the env gene of Mason-Pfizer monkey virus: effects on protein transport and SU–TM association. J.Virol. 66, 3466–3475.
Campos-Olivas, R., Newman, J.L., Summers, M.F., 2000. Solution structure and dynamics of the Rous sarcoma virus capsid protein and comparison with capsid proteins of other retroviruses. J. Mol. Biol. 296, 633–649.
Cornilescu, C.C., Bouamr, F., Yao, X., Carter, C., Tjandra, N., 2001. Structural analysis of the N-terminal domain of the human T-cell leukemia virus capsid protein. J. Mol. Biol. 306, 783–797.
Forshey, B.M., von Schwedler, U., Sundquist, W.I., Aiken, C., 2002. Formation of a human immunodeficiency virus type 1 core of optimal stability is crucial for viral replication. J. Virol. 76, 5667–5677.
Gamble, T.R., Yoo, S.H., Vajdos, F.F., vonSchwedler, U.K., Worthylake, D.K., Wang, H., McCutcheon, J.P., Sundquist, W.I., Hill, C.P., 1997. Structure of the carboxyl-terminal dimerization domain of the HIV-1 capsid protein. Science 278, 849–853.
Gamble, T.R., Vajdos, F.F., Yoo, S., Worthylake, D.K., Houseweart, M., Sundquist, W.I., Hill, C.P., 1996. Crystal structure of human cyclophilin A bound to the amino-terminal domain of HIV-1 capsid. Cell 87, 1285–1294.
Ganser-Pornillos, B.K., von Schwedler, U.K., Stray, K.M., Aiken, C., Sundquist, W.I., 2004. Assembly properties of the human immunodeficiency virus type 1 CA protein. J. Virol. 78, 2545–2552.
Ganser-Pornillos, B.K., Cheng, A., Yeager, M., 2007. Structure of full-length HIV-1 CA: a model for the mature capsid lattice. Cell 131, 70–79.
Gitti, R.K., Lee, B.M., Walker, J., Summers, M.F., Yoo, S., Sundquist, W.I., 1996. Structure of the amino-terminal core domain of the HIV-1 capsid protein. Science 273, 231–235.
Gross, I., Hohenberg, H., Huckhagel, C., Krausslich, H.G., 1998. N-terminal extension of human immunodeficiency virus capsid protein converts the in vitro assembly phenotype from tubular to spherical particles. J. Virol. 72, 4798–4810.
Jin, Z., Jin, L., Peterson, D.L., Lawson, C.L., 1999. Model for lentivirus capsid core assembly based on crystal dimers of EIAV p26. J. Mol. Biol. 286, 83–93.

Khorasanizadeh, S., Campos-Olivas, R., Summers, M.F., 1999. Solution structure of the capsid protein from the human T-cell leukemia virus type-I. J. Mol. Biol. 291, 491–505.

Kingston, R.L., Fitzon-Ostendorp, T., Eisenmesser, E.Z., Schatz, G.W., Vogt, V.M., Post, C.B., Rossmann, M.G., 2000. Structure and self-association of the Rous sarcoma virus capsid protein. Struc. Fold. Des. 8, 617–628.

Leschonsky, B., Ludwig, C., Bieler, K., Wagner, R., 2007. Capsid stability and replication of human immunodeficiency virus type 1 are influenced critically by charge and size of Gag residue 183. J. Gen. Virol. 88, 207–216.

Momany, C., Kovari, L.C., Prongay, A.J., Keller, W., Gitti, R.K., Lee, B.M., Gorbalenya, A.E., Tong, L., McClure, J., Ehrlich, L.S., Summers, M.F., Carter, C., Rossmann, M.G., 1996. Crystal structure of dimeric HIV-1 capsid protein. Nat. Struct. Biol 3, 763–770.

Mortuza, G.B., Haire, L.F., Stevens, A., Smerdon, S.J., Stoye, J.P., Taylor, I.A., 2004. High-resolution structure of a retroviral capsid hexameric amino-terminal domain. Nature 431, 481–485.

Mortuza, G.B., Dodding, M.P., Goldstone, D.C., Haire, L.F., Stoye, J.P., Taylor, I.A., 2008. Structure of B-MLV capsid amino-terminal domain reveals key features of viral tropism, Gag assembly and core formation. J. Gen. Virol. 376, 1493–1508.

Nandhagopal, N., Simpson, A.A., Johnson, M.C., Francisco, A.B., Schatz, G.W., Rossmann, M.G., Vogt, V.M., 2004. Dimeric Rous sarcoma virus capsid protein structure relevant to immature Gag assembly. J. Mol. Biol. 335, 275–282.

Newman, R.M., Hall, L., Connole, M., Chen, G.L., Sato, S., Yuste, E., Diehl, W., Hunter, E., Kaur, A., Miller, G.M., Johnson, W.E., 2006. Balancing selection and the evolution of functional polymorphism in Old World monkey TRIM5{alpha}. Proc. Natl. Acad. Sci. U. S. A. 103, 19134–19139.

Parker, S.D., Hunter, E., 2001. Activation of the Mason-Pfizer monkey virus protease within immature capsids in vitro. Proc. Natl. Acad. Sci. U. S. A. 98, 14631–14636.

Pettit, S.C., Henderson, G.J., Schiffer, C.A., Swanstrom, R., 2002. Replacement of the P1 amino acid of human immunodeficiency virus type 1 Gag processing sites can inhibit or enhance the rate of cleavage by the viral protease. J. Virol. 76, 10226–10233.

Rayne, F., Bouamr, F., Lalanne, J., Mamoun, R.Z., 2001. The NH2-terminal domain of the human T-cell leukemia virus type 1 capsid protein is involved in particle formation. J. Virol. 75, 5277–5287.

Rumlova, M., Ruml, T., Pohl, J., Pichova, I., 2003. Specific in vitro cleavage of Mason-Pfizer monkey virus capsid protein: evidence for a potential role of retroviral protease in early stages of infection. Virology 310, 310–318.

Rumlova-Klikova, M., Hunter, E., Nermut, M.V., Pichova, I., Ruml, T., 2000. Analysis of Mason-Pfizer monkey virus gag domains required for capsid assembly in bacteria: role of the N-terminal proline residue of CA in directing particle shape. J. Virol. 74, 8452–8459.

Stansell, E., Apkarian, R., Haubova, S., Diehl, W.E., Tytler, E.M., Hunter, E., 2007. Basic residues in the Mason-Pfizer monkey virus Gag matrix domain regulate intracellular trafficking and capsid-membrane interactions. J. Virol. 81, 8977–8988.

Strambio-de-Castillia, C., Hunter, E., 1992. Mutational analysis of the major homology region of Mason-Pfizer monkey virus by use of saturation mutagenesis. J. Virol. 66, 7021–7032.

von Schwedler, U.K., Stemmler, T.L., Klishko, V.Y., Li, S., Albertine, K.H., Davis, D.R., Sundquist, W.I., 1998. Proteolytic refolding of the HIV-1 capsid protein amino-terminus facilitates viral core assembly. Embo. J. 17, 1555–1568.

von Schwedler, U.K., Stray, K.M., Garrus, J.E., Sundquist, W.I., 2003. Functional surfaces of the human immunodeficiency virus type 1 capsid protein. J. Virol. 77, 5439–5450.